Control of Chaotic Taylor-Couette Flow with Time-Delayed Feedback

O. Lüthje, S. Wolff, and G. Pfister

Institut für Experimentelle und Angewandte Physik, Universität Kiel, Olshausenstraße 40, D-24098 Kiel, Germany

(Received 9 August 2000)

We demonstrate that unstable periodic orbits embedded in the experimental chaotic attractor determined by the Taylor-Couette flow can be stabilized with a time-delay autosynchronization algorithm. The optimal parameters of the feedback and their dependence on the control parameter are shown as experimental results.

DOI: 10.1103/PhysRevLett.86.1745 PACS numbers: 05.45.Gg, 47.20.−k, 47.52.+j

There are several methods that deal with the problem of stabilization of chaotic dynamics to periodic orbits. The method proposed by Ott, Grebogi, and Yorke (OGY) [1] is based on the determination of stable and unstable directions in a Poincaré section. This technique applies small perturbations to an accessible control parameter in discrete time intervals. It has been applied to some experimental systems [2–5] including a stabilization of pattern dynamics in a Taylor vortex flow with hourglass geometry [6]. Another method of chaos control is known as time-delayed autosynchronization (TDAS) and has been proposed by Pyragas [7]. This technique uses a continuous time-delayed feedback. It has been shown to be an efficient method and has been applied in numerical simulations as well as in experiments [8–12].

A control algorithm that uses time-delayed feedback requires less previous information about the system behavior than methods based on the OGY algorithm. Unstable periodic orbits (UPOs) of the dynamical system can be stabilized with an appropriate feedback determined by the period of the UPO. From the theoretical point of view the stabilization with TDAS has not been fully understood. Important progress has been made by applying Floquet theory, leading to some limitations of the technique as the success of TDAS depends on the torsion of neighboring trajectories in the phase space [13].

We report in this Letter that we have succeeded in stabilizing the unstable period-one and period-two orbits in a spatially extended flow experiment, the Taylor-Couette system.

The Taylor-Couette flow consists of a viscous fluid between two concentric cylinders with radii r_i (inner cylinder) and r_o (outer cylinder). While the inner cylinder rotates, the outer cylinder and the end plates are at rest. The external control parameter is the Reynolds number, defined as $\mathrm{Re} = (2\pi f d r_i)/\nu$, where f denotes the rotation frequency of the inner cylinder, $d = r_o - r_i$ is the gap width, and $\nu = 11.8$ cS is the kinematic viscosity of the silicon oil, used as fluid for the experiment. The given experimental parameters describing the experimental apparatus are $r_i = 12.5$ mm, $r_a = 25$ mm, $\Gamma = 0.42$, and a lid inclination of 0.39°, which causes a slight asymmetry of the system geometry. The aspect ratio $\Gamma = L/d$ is defined as the ratio of cylinder height L and the gap width d. For the low-dimensional dynamics that are the topic of this paper, the global dynamics can be derived from a scalar variable [14]. In our case the local axial velocity component $v_z = v_z(t, \mathbf{x})$ is measured by a real-fringe laser-Doppler velocimeter (LDV) and recorded by a phase-locked-loop analog tracker. This technique provides a precise measurement of one velocity component of the flow at a chosen point of measurement. After filtering with a bandpass the signal is fed into an analog-to-digital converter with 14-bit resolution. The resulting digital signal is used for the feedback calculation.

As long as the Reynolds number Re is very small, the flow is a circular shear flow, called the *circular Couette flow*. If Re is increased to a quasicritical value $\mathrm{Re}_{\mathrm{TVF}}$, the flow becomes centrifugally unstable and assumes a regular cellular vortex structure in which annular vortices with alternating flow direction enclose the inner cylinder. This flow is called the *Taylor vortex flow* (TVF). The number and geometry of these vortices depend on the aspect ratio $\Gamma = L/d$ [15].

Numerical approaches to flow experiments are based on the Navier-Stokes equations and hence lead to an infinite-dimensional phase space. As a result there is no model for the dynamics of the Taylor-Couette system due to the large number of possible solutions. Although the steady solutions correspond to highly correlated system states, we speak of a spatially extended system, because time constants occur that are caused by the propagation of perturbations, e.g., changes of the control parameter. However, small values of the aspect ratio ($\Gamma \leq 1$) reduce the number of steady solutions, because only states with one or two Taylor vortices are possible. For this system of reduced complexity, the main bifurcations have been found consistently both by numerical and by experimental investigations [14]. The first vortex structure that occurs is a symmetric two-cell state ($2s$). On increasing the Reynolds number the two-cell state $2s$ branches into two equivalent single-cell state modes $1a$, each with a large main vortex near the top or the bottom, respectively, and a small weak vortex. For higher Reynolds numbers there is a restabilized symmetric two-cell state $2s^*$, which shows a time-periodic Hopf bifurcation. With increasing Reynolds

number the $2s^*$ state may undergo a transition to chaos via period doubling or intermittency until it loses stability to the one-cell states. The chaotic attractors used for this investigation arise from period-doubling cascades. Such scenarios have been found only in experiments with a small inclination of one end plate. The dependence of the transition to chaos on the boundary conditions for small values of Γ is discussed in [16].

Thus we have a spatially extended flow experiment, the dynamics of which is at least roughly understood. This, combined with a precise measurement technique, enables us to apply the chosen feedback control method.

The feedback $F(t)$ for the control process is proportional to the difference $D(t)$ between the signal $v_z(t)$ provided by the LDV and the delayed signal $v_z(t - \tau)$ [7],

$$F_\tau(t) = k[v_z(t) - v_z(t - \tau)] = kD(t). \quad (1)$$

The perturbation $F(t)$ is applied to the cylinder rotation frequency f_0 (Fig. 1), which corresponds to a control parameter $\mathrm{Re}_0 = \mathrm{Re}(f_0)$:

$$f(t) = f_0 + F(t). \quad (2)$$

We restrict the absolute value of the perturbation to $F_0 = 0.127$ Hz (which corresponds to $|\Delta\mathrm{Re}| = 10.8$ for the given viscosity):

$$F(t) = \begin{cases} F_0 & F_\tau(t) > F_0 \\ F_\tau(t) & -F_0 \le F_\tau(t) \le F_0 \\ -F_0 & F_\tau(t) < -F_0 \end{cases}. \quad (3)$$

As explained in [7], the restriction does not change the result, if control is achieved. In the given case of multistability the restriction of imposing a maximum absolute value F_0 of the perturbation is important to keep the system from switching from the two-cell to a one-cell state.

If $v_z(t)$ is a periodic signal corresponding to a periodic solution $y_i(t)$ of the system and $\tau = T_i$ the corresponding period, the perturbation $F(t)$ becomes zero. This means that $y_i(t)$ is a solution of both the perturbed and the unchanged system. As the weight k associates with two completely different variables, its absolute value and unit are irrelevant. The absolute values of k that appear in the following text are used to allow a comparison with the results for larger parameter ranges.

Chaos control can be achieved by choosing an appropriate value of the adjustable weight k. Specific values of k provide a stabilization of the desired UPO [represented by the solution $y_i(t)$], which is embedded in the strange attractor. These optimal values strongly depend on the control parameter and the chosen UPO; this will be discussed later.

The choice of the experimental parameters provides a $2s^*$ state with a clear period doubling with increasing Re, as shown in Fig. 2. The phase space reconstruction for a period-one solution [Fig. 2(a)], a period-two solution [Fig. 2(b)], and the chaotic attractor [Fig. 2(c)] is shown. The reconstruction has been performed by time-delay embedding as proposed by Takens [17], such that a vector in the embedding space is given by

$$\vec{x}(t) = v_z(t), v_z(t + \tau_{\mathrm{rec}}), \ldots, v_z(t + \tau_{\mathrm{rec}}[m - 1]), \quad (4)$$

where τ_{rec} is the reconstruction delay time and m is the embedding dimension.

Figure 3 shows the result of applying the control algorithm with delay $\tau = 1.72s$, weight $k = 0.062$, and control parameter $\mathrm{Re} = 567$. The value of the selected delay

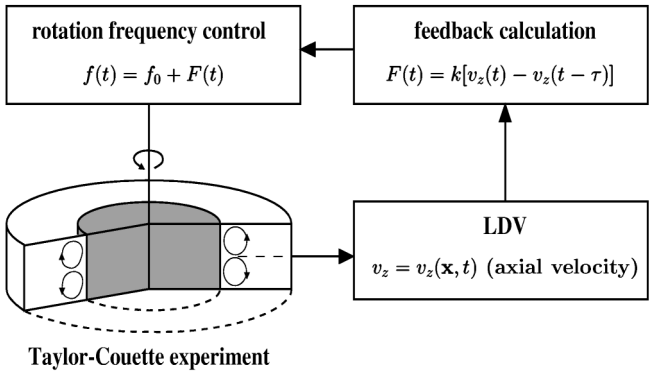

FIG. 1. Illustration of the feedback loop: The feedback is instantaneously calculated and applied to the rotation frequency of the inner cylinder of the Taylor-Couette flow experiment.

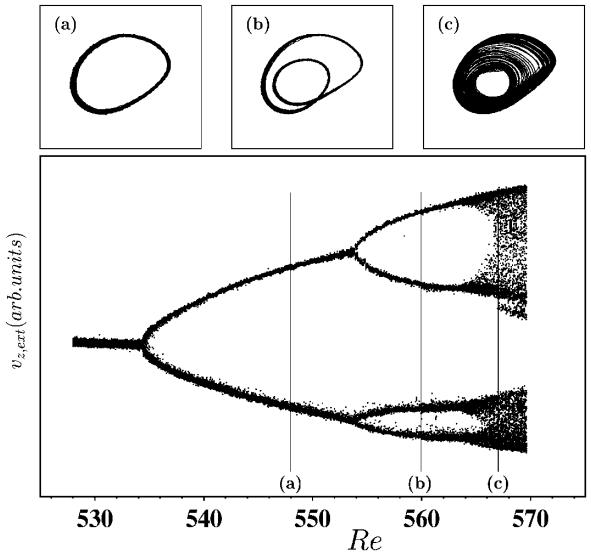

FIG. 2. Experimental bifurcation diagram of the restabilized two-cell state. Extrema of the axial velocity v_z are plotted against the Reynolds number Re. For illustration of the period doubling, the phase space reconstruction of the attractor is shown for (a) $\mathrm{Re} = 548$ with a resulting period of $T = T_0$, (b) $\mathrm{Re} = 560$ with $T = 2T_0$, and (c) $\mathrm{Re} = 567$ showing the chaotic attractor.

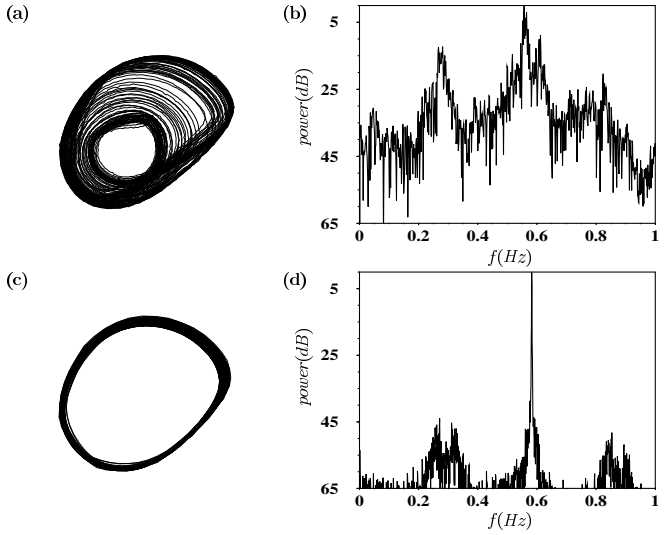

FIG. 3. Experimental data showing the phase space reconstruction of the strange attractor (a) of the unperturbed system for Re = 567 and (c) the result of the chaos control algorithm for $k = 0.062$, $\tau = 1.72$. (b),(d) The corresponding power spectra in dB with respect to the main fast-Fourier transform channel.

time τ is chosen near the main period of the system and corresponds to the period-one UPO of the system. As a result the UPO becomes stable. The phase space reconstruction [Fig. 3(c)] is comparable to the stable period-one solution for Re = 548, shown in Fig. 2(a).

When starting the control process the state of the system is in general not in the neighborhood of the UPO selected by the choice of τ. As a result there is a large difference $D(t) = v_z(t) - v_z(t - \tau)$ between the present and the time-delayed signal at this stage of the process. Maximum values of the absolute difference $|D(t)|$ are of the same magnitude as the amplitude of the signal v_z itself. After a transient process, $|D(t)|$ stays lower than 15% of the signal amplitude. This process of targeting the trajectory onto the desired orbit is accomplished in less than $250T_0$ for optimal values of k and τ. A small deviation from these optimal parameters leads to a higher residual control signal but it does not increase the needed time to more than $500T_0$ s. The power spectrum of the experimental control result [Fig. 3(d)] still shows a small peak at $f_0/2$, originating from the small deviation of the selected UPO. An investigation of the dependence of the mean difference $\overline{|D(t)|}$ on k and τ, discussed below, will show that this is the best result one can attain for the given experimental setup.

We now discuss the dependence of the mean difference $\overline{|D(t)|}$ on k. It appears that control of the period-one orbit can be achieved in a narrow interval of the weight k, as shown in Fig. 4(b). Each value $\overline{|D(t)|} = \overline{|y(t) - y(t - \tau)|}$ has been calculated for 40 000 points at a sampling rate of 50 Hz after 800 s lead time. This large value of the lead time ensures that control has certainly been achieved if possible. Figure 4(a) shows

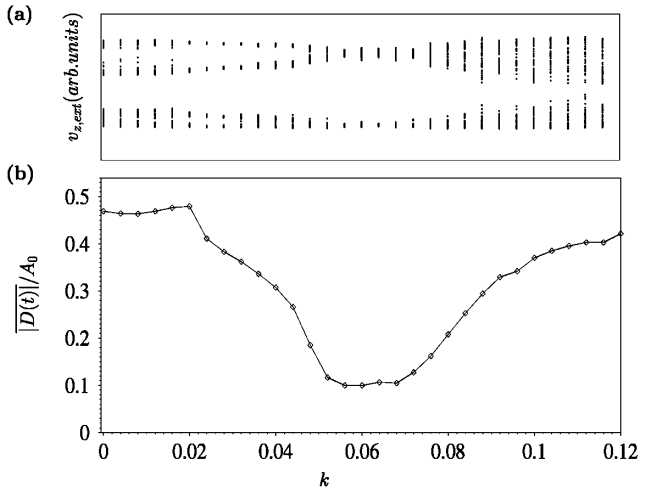

FIG. 4. Experimental results for the dependence of the period-one control result on k for a delay time of $\tau = T_0 = 1.72$ s. (a) The extrema of v_z and (b) the corresponding mean difference $\overline{|D(t)|}$.

the corresponding extrema of the signal v_z. One can observe that the controlled system loses stability via period doubling with decreasing k.

Figure 5(b) shows the dependence of $\overline{|D(t)|}$ on τ for the stabilization of the period-one UPO. If there is a small deviation ($\Delta\tau = \tau - T_0$) between the delay and the period of the UPO, the resulting control signal also has a period of T_0, while its phase shift and amplitude depend on $\Delta\tau$. Consequently, the control signal $F(t)$ applies a slight modulation to the cylinder rotation frequency, if the stabilization is not affected by the residual feedback. For a stable sine wave the difference can be calculated to

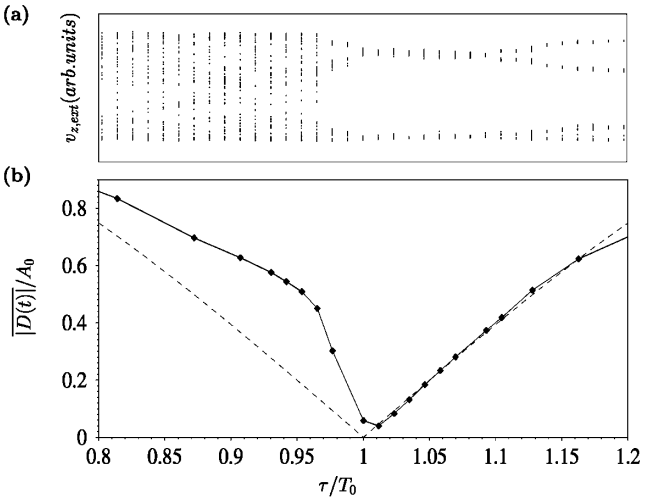

FIG. 5. Experimental results for the dependence of the period-one control result on the delay time τ for a weight $k = 0.065$. (a) The extrema of v_z and (b) the mean difference $\overline{|D(t)|}$. The dotted line shows the corresponding $\overline{|D(t)|}$ for a sine wave [Eq. (5)].

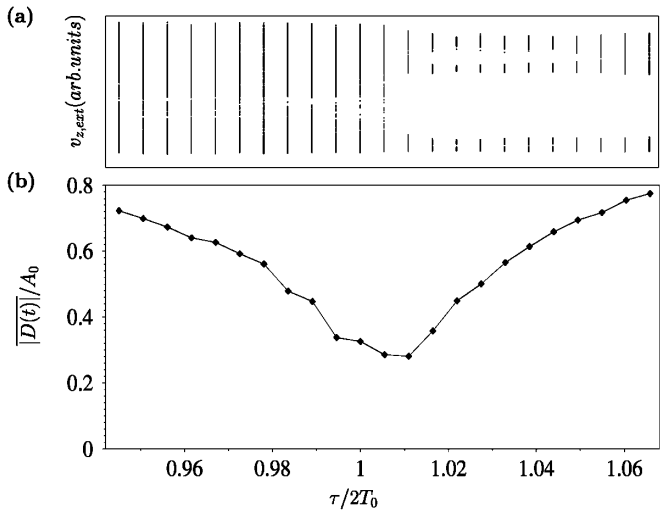

FIG. 6. Experimental results for the dependence of the period-two control result on the delay time τ for a weight $k = 0.065$. (a) The extrema of v_z and (b) the mean difference $\overline{|D(t)|}$.

$$\overline{|D(t)|}\,(\tau) = \frac{2v_0}{\pi}\sqrt{2 - 2\cos\frac{2\pi}{T_0}\,\tau} \qquad (5)$$

using Eq. (1), where v_0 is the amplitude of the oscillation. The good agreement of the experimental results for a successful stabilization with this optimal dependence described by Eq. (5) can be seen in Fig. 5(b) for $1 > \tau/T_0 > 1.1$. Figure 5(a) shows that, in this range of τ/T_0, stability can be reached in spite of the residual feedback. The controlled system loses stability via period doubling with increasing $\Delta\tau$.

Figure 6(b) shows the dependence of $\overline{|D(t)|}$ on τ for the stabilization of the period-two UPO. As Fig. 6(a) shows, the stabilization can be reached for a delay time larger than $2T_0$ and a larger residual mean difference $\overline{|D(t)|}$ than the corresponding values for the stabilization of the period-one UPO.

Figure 5(b) shows that the minimum value of $\overline{|D(t)|}$ does not occur precisely at $\tau/T_0 = 1$, as one would expect. This, in addition to the nonvanishing feedback for $t \to \infty$, shows that the optimal performance cannot be reached, in contrast to numerical simulations of TDAS. There are two possible explanations for this insufficiency for the case of a spatially extended flow experiment. The first possible explanation is given by the presence of measurement noise. This noise is an unwanted perturbation fed back into the system. In comparison with numerical results, this can be a reason for the nonvanishing feedback values $F(t)$ even after stabilization has been reached, but this effect does not explain the asymmetry of $\overline{|D(t)|}$ with respect to $\tau/T_0 = 1$. The second possible explanation is given by the propagation time of the perturbation within the fluid, which leads to an additional delay time and causes noninstant feedback at the chosen point of measurement. The influence of an additional delay on the TDAS control method is discussed in [18]. In the case of a linear delay, such as a control loop latency, the interval of the weight k, for which stabilization can be reached, gets smaller with an increasing additional delay. In general the additional delay shifts the points of frequency splitting which delimit the interval of stabilizing parameter values k and τ.

We have applied the TDAS scheme successfully to a spatially extended flow experiment, the Taylor-Couette system. Both the period-one and the period-two UPOs have been stabilized with an appropriate feedback. The parameter ranges in which control is possible have been discussed, as well as possible explanations for the residual feedback.

The dependence of the quality of the control on the additional delay, caused by the propagation time within the fluid, will be a topic of further investigation. It will also be beneficial to apply chaos control methods on other modes of the Taylor-Couette flow.

We thank the Deutsche Forschungsgemeinschaft for their support (research Grant No. PF-210-6).

[1] E. Ott, C. Grebogi, and J. Yorke, Phys. Rev. Lett. **64**, 1196 (1990).
[2] W. Ditto, S. Rauseo, and M. Spano, Phys. Rev. Lett. **65**, 3211 (1990).
[3] E. Hunt, Phys. Rev. Lett. **67**, 1953 (1991).
[4] R. Roy *et al.,* Phys. Rev. Lett. **68**, 1259 (1992).
[5] P. Parmananda, P. Sherard, R. Rollins, and H. Dewald, Phys. Rev. E **47**, 3003 (1993).
[6] R. Wiener, D. C. Dolby, G. Gibbs, B. Squires, T. Olsen, and A. Smiley, Phys. Rev. Lett. **83**, 2340 (1999).
[7] K. Pyragas, Phys. Lett. A **170**, 421 (1992).
[8] J. Socolar, D. Sukow, and D. Gauthier, Phys. Rev. E **50**, 3245 (1994).
[9] K. Pyragas, Phys. Lett. A **206**, 323 (1995).
[10] R. de Korte, J. Schouten, and C. van den Bleek, Phys. Rev. E **52**, 3358 (1995).
[11] A. Namajũnas, K. Pyragas, and A. Tamaševičius, Phys. Lett. A **204**, 255 (1995).
[12] H. Nakajima and Y. Ueda, Phys. Rev. E **58**, 1757 (1998).
[13] W. Just *et al.,* Phys. Rev. Lett. **78**, 203 (1997).
[14] G. Pfister, H. Schmidt, K. Cliffe, and T. Mullin, J. Fluid Mech. **191**, 1 (1988).
[15] *Lecture Notes in Physics: Physics of Rotating Fluids,* edited by C. Egbers and G. Pfister (Springer, New York, 2000).
[16] T. Buzug, J. von Stamm, and G. Pfister, Phys. Rev. E **47**, 1054 (1993).
[17] F. Takens, in *Lecture Notes in Mathematics: Dynamical Systems and Turbulence (Warwick 1980),* edited by D. A. Rand and L.-S. Young (Springer, New York, 1981), Vol. 898, pp. 366–381.
[18] W. Just, D. Reckwerth, E. Reibold, and H. Benner, Phys. Rev. E **59**, 2826 (1999).